FPRINT-94-38

Fermilab Library
0 1160 0039003 3

UNIVERSITA' DEGLI STUDI DI MILANO

DIPARTIMENTO DI FISICA
GRUPPO ALTE ENERGIE

FERMILA
AUG 19
LIBR

HADRO AND PHOTOPRODUCTION OF CHARMS AT FIXED TARGET

G. BELLINI
Dipartimento di Fisica dell'Universita' and Istituto Nazionale di Fisica Nucleare - Sezione di Milano - Via Celoria, 16 - Milano - Italy

Milan U.
INFN, Milan

NAME	I D No	M.S.

RETURN TO FERMILAB LIBRARY

HADRO AND PHOTOPRODUCTION OF CHARMS AT FIXED TARGET

G. Bellini
Dipartimento di Fisica - Universita' di Milano
Istituto Nazionale di Fisica Nucleare - Sezione di Milano
Via Celoria, 16 - 20133 Milano - Italy

The results summarized in this paper concern only recent data, obtained at fixed target on open charms, which can compete with e^+e^- data and can be directly and significantly compared with the theoretical models. They have been collected at photon and hadron beams at CERN and FNAL (and at IHEP) in various experiments, listed in Table I.

This paper consists of six sections, devoted to the following topics: production mechanisms, new decay channels of charmed baryons, lifetimes, charm hadronic decays, charm semileptonic decays, CP violation study.

Table I

Experiments	Beam	Energy (GeV)
NA 14/2	γ	95*
E691	γ	145*
E687	γ	220*
NA32	π	230
WA75	π	270
E769	π	250
WA78	π	320
WA82/92	π	340
E653	π	500/600
E791	π	500
WA89	Σ	330
EXCHARM	n	40

* For photon beams the quoted value is the average γ energy.

1. Production mechanisms

The more important parameters, which are experimentally measured to study the production mechanisms, are the following:

- the total cross sections;
- x_F, p_t and the leading particle effect, in the inclusive measurements;

- the acopianarity angle, $p_t(D\bar{D}), \Delta Y, M(D\bar{D}), \frac{E_D + E_{\bar{D}}}{E_{beam}}$, in the double tag events.

The experimental data are compared with:

i) the previsions of the perturbative QCD [photon-gluon fusion; gluon-gluon fusion] calculated in the Leading Order (LO) and Next-to-Leading Order (NLO) approximations[1,2,3,4,5];

ii) the simulations of LUND-PYTHIA code. In this programme the photon-gluon and the gluon-gluon fusion model is applied at the LO approximation with NLO corrections incorporated in the leading logarithmic approximation (Shower model). In addition the fragmentation mechanism is included using the string model;

iii) the simulations of HERWIG code. This programme is very similar to the previous one, but the fragmentation mechanism is simulated by means of the cluster model.

The perturbative QCD calculation is strongly sensitive to the renormalization scale μ. It is generally assumed equal to M_c and it is allowed to range between $\frac{M_c}{2}$ and $2M_c$.

1.1. Total cross sections

The NLO corrections give important contributions to the cross sections especially in the hadroproduction case. In Fig. 1 the total cross sections $\sigma(\gamma N \to c\bar{c})$ and $\sigma(\pi N \to c\bar{c})$, measured at various energies, are fitted using the NLO perturbative QCD. In both cases the best fit gives $\mu = M_c = 1.5$ GeV, which is a very reasonable value. The theoretical errors are very large; they are due to the uncertainties on Λ_{QCD}, M_c and higher order corrections.

1.2 Inclusive measurements

x_F - The differential cross sections $\frac{d\sigma}{dx_F}$ as measured by NA14[6], E691[7], E687, are in good agreement each to other[8]. They show a maximum at ~0.2, while the NLO calculations (which differ very little from the LO approximation) give a distribution with a maximum at 0.5.

This disagreement is interpreted as due to the fragmentation effects, which shift the experimental distribution to lower x_F values.

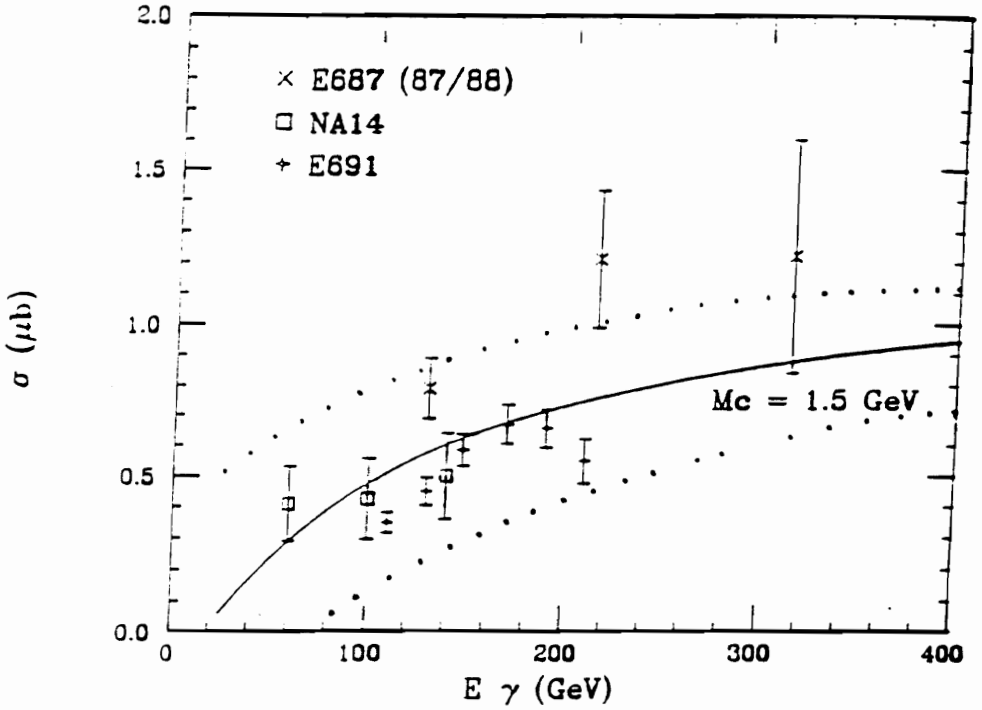

Fig. 1a

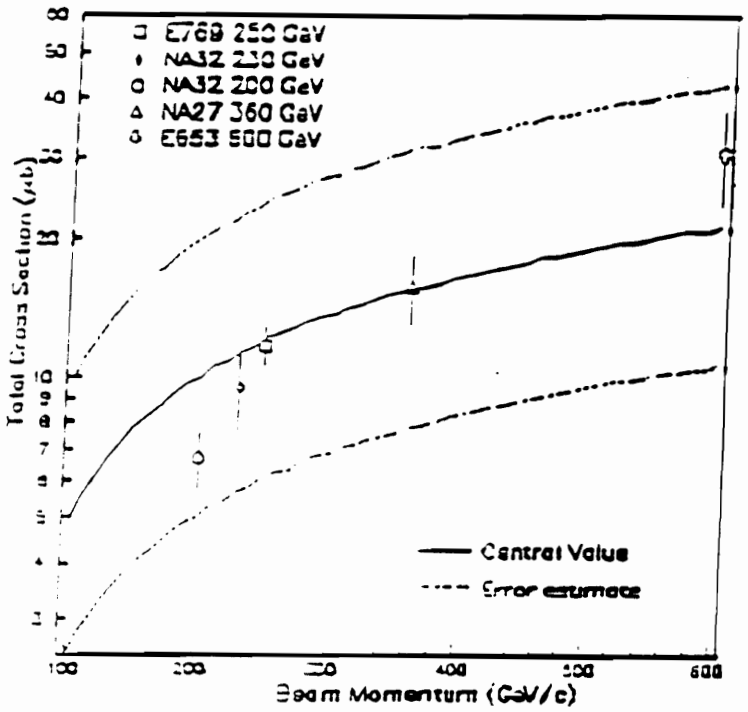

Fig. 1b

Fig. 1 - Total cross sections of $c\bar{c}$ production at various energies.

a) Photon beam. The full line curve is the NLO calculation with $\mu = M_c = 1.5\ GeV$ central value; the error band is limited by the dotted curves.

b) π beams. The legenda of the theoretical curves are the same as in Fig. 1a.

On the other hand in hadroproduction the agreement between experimental results and NLO previsions is quite good. The experimental distributions are well fitted by $\frac{d\sigma}{dx_F} = k(1-x_F)^n$, where $n = 3-4$ for incident π and ~5-8 for baryon beams[8]. This different behaviour in photon and hadroproduction can be interpreted as an effect of dragging of the charm quark by the projectile quark spectator (the so called color drag).

p_t - Also in this case the NLO corrections, with respect to the LO approximation, are very small.

In photoproduction the p_t distributions are well reproduced by the exponential:

$$\frac{dN}{dp_t^2} = A\exp(ap_t^2 + bp_t^4) \qquad (1)$$

$<p_t^2>$ and the best fit values for a and b, as obtained by E687 and E691, are summarized in Table II.

Table II

	a	b	$<p_t^2>$ $(GeV/c)^2$
E687	-0.85±0.02	0.03±0.01	1.51±0.02
E691	-1.07±0.05	0.04±0.01	1.16±0.04

There is a basic agreement between the values displayed in Table II and the NLO expectations[9], if we assume a mass value $M_c = 1.2\ GeV$, which, on the other hand, seems too low.

The hadroproduction experiments use an exponential $\exp(-bp_t^2)$ to fit the lower part of the spectrum. In order to fit also the higher values, a distribution like (1) has to be preferred or an exponential like $\exp(-bp_t)$, as used by WA82 and E769[10]. The average $<P_T>$ value (~1 GeV) is well reproduced by the LO calculations.

Leading. In the production of charmed states a kinematic correlation may arise if a light quark in an initial state particle is transferred to the produced charm meson. This could result in a leading particle effect, which can be studied by analyzing the kinematical behaviour of the produced particles sharing a valence quark with the beam. The asymmetry parameter (2) is measured as function of x_F and p_t.

$$A = \frac{N(leading - N(nonleading)}{N(leading) + N(nonleading)} \qquad (2)$$

The asymmetry parameter A, integrated over $x_F > 0$, gives a very small effect. On the other hand, recently WA82[11] and E769[12] measured A as a function of x_F and p_t. The asymmetry is growing up as x_F increases, reaching values ≥ 0.5 for $x_F \geq 0.6$. If we combine the data of the two experiments the effect is statistically significant (see Fig. 2).

A similar study of A vs p_t^2 gives a flat distribution, consistent with zero.

In the photon gluon fusion c and $\bar{c}$ quarks are produced with the same cross section if we limit the calculations to the LO. In the NLO the $\bar{c}$ is slightly favoured with respect to the c quark, giving rise to a small asymmetry (Fig. 2), which is positive for

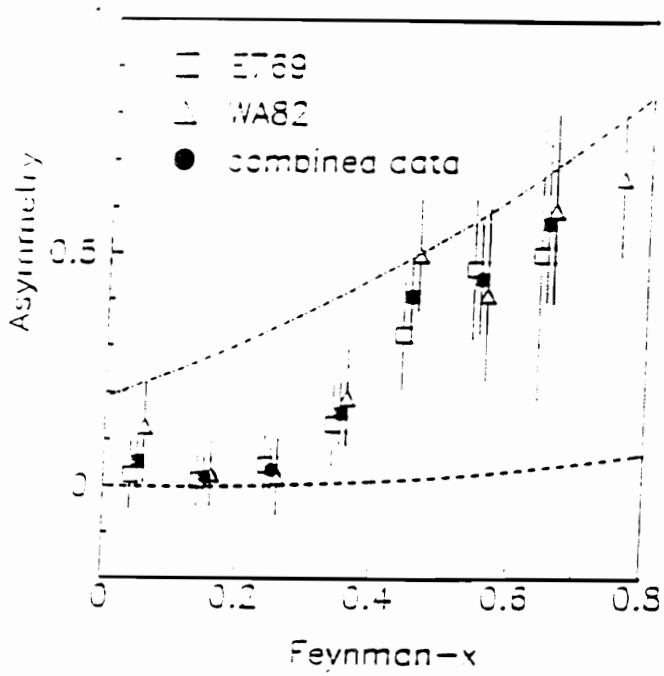

Fig. 2 - The leading particle asymmetry vs x_F.. The dashed line is the NLO calculation. The dashed-dotted line is the LUND-PYTHIA simulation (see text);

charged D and D^* containing a $\bar{c}$ quark[11]. But the expected asymmetry is definitively much more lower than what it is experimentally observed.

Possible explanations of this discrepancy are based upon non-perturbative effects, as an effect of dragging of the charmed quarks due to an interaction with the spectator quark. This effect has been implemented in LUND-PYTHIA program. The trend agrees with the experimental results, even if the predicted A values are too high (Fig. 2).

D^*'s. E769 has studied the inclusive distributions for D^*'s and have compared them to D's[13]. These distributions could be different because the hadronization process can differ between pseudoscalar and vector mesons. The x_F, p_t distributions and the leading

particle effects have been studied and appear to be consistent, within the errors, with the results obtained for D's.

A dependence. As it is well known the cross section dependence on atomic mass of the target material is parametrized as A^{α}. New results have been obtained recently by WA82[14] and E769[15], both using a π beam. E769 analyzes separately the D and D^* samples. The results are displayed in Table III.

Table III

Expt.	p(beam) (GeV)	produced charm	α	X_F range
WA82	340	D^0, D^+	0.92±0.06	>0.0
E769	250	D^0, D^+	1.0±0.05±0.02	>0.0
E769	250	D^*	1.0±0.007±0.02	>0.0

1.3 Correlations

The $D\bar{D}$ correlations can be studied using samples of double tag events, where both the D's are reconstructed. The D decay channels taken into account are the golden modes: $K\pi, K\pi\pi, K\pi\pi\pi$. Significant statistics of double tag events have been obtained by the experiments listed in Table IV.

Table IV

Expt	Incident particles	E_{beam}	Sample of double tag events
E687	γ	220	325
NA14/2	γ	92	22
NA32	π	230	557
WA75	π	270	177

In addition, more recently, WA92[16] selected a sample of 81 events, where only one D is fully reconstructed, while the second secondary vertex is identified and its possible correlation with strange particle decays is ruled out. For this sample only the $D\bar{D}$ acoplanarity angle can be measured.

$D\bar{D}$ acoplanarity angle.- It is the angle between the D and $\bar{D}$ flight directions in a plane transverse to the beam axis. In a simple LO approach this angle has to be $\equiv \pi$. The radiative corrections introduces an important smearing, which agrees with the experimental distribution in photoproduction[3,17] (see Fig. 3a), but is definively inadequate to reproduce the data obtained in hadroproduction (see Fig. 3b - the data are from NA32, but WA75 and E653 give very similar distributions).

The experimental data can be well reproduced by the LUND simulations, where the intrinsic p_t of the incident gluon is modelled as a Gaussian distribution with $\sigma \sim 1$GeV/c for photoproduction and ~1.7 for hadroproduction. But a $p_t \sim 1.7$ GeV/c seems definitively too high.

Very recently WA92 measured a less smeared distribution (Fig. 3c), which can be reproduced by a simple LO approach with in addition a $\sigma(p_t^{gluon}) = 1\ GeV/c$.

If this last result is true, it is possible to foresee a common explanation for photon and hadroproduction. But, first of all, we have to understand the discrepancy between WA92 and the other hadroproduction experiments (the selected sample represents only the 20% of the total statistics collected by WA92).

Δy - It is the difference between the D and $\bar{D}$ pseudorapidities. It shows a reasonable agreement with the NLO approach, both in photoproduction and hadroproduction.
Good agreement has been obtained also by comparing the experimental distribution obtained by E687 and the LUND calculations, with $\sigma(p_t^{gluon}) = 0.44\ GeV/c$.

$p_t(D\bar{D})$-It is the transverse momentum of the $D\bar{D}$ pair. The experimental results seem larger than the Lund prediction with $\sigma(p_t^{gluon}) = 0.44$;

$M(D\bar{D})$-It is the invariant mass of the $D\bar{D}$ pairs. The situation is very similar to that of $p_t(D\bar{D})$.

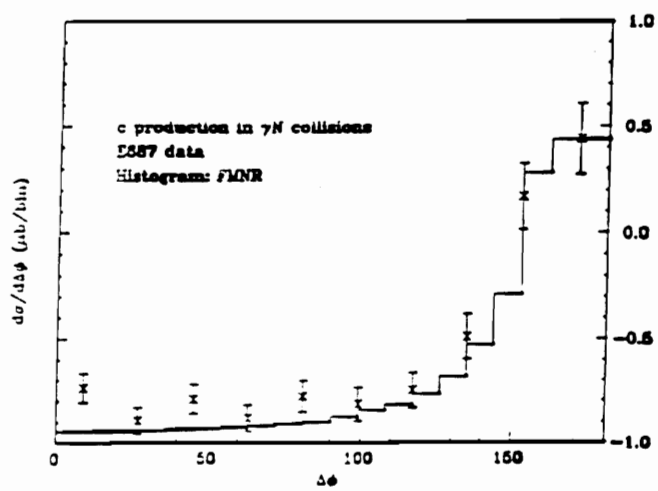

Fig. 3a

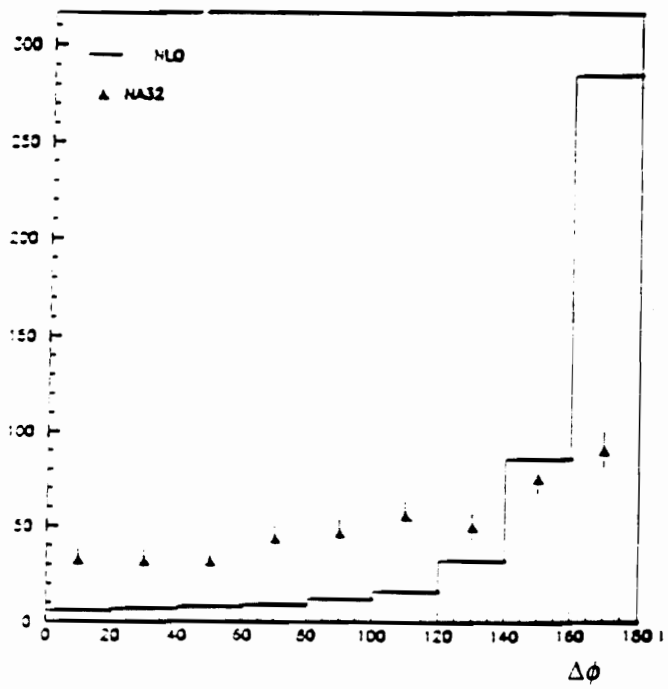

Fig. 3b

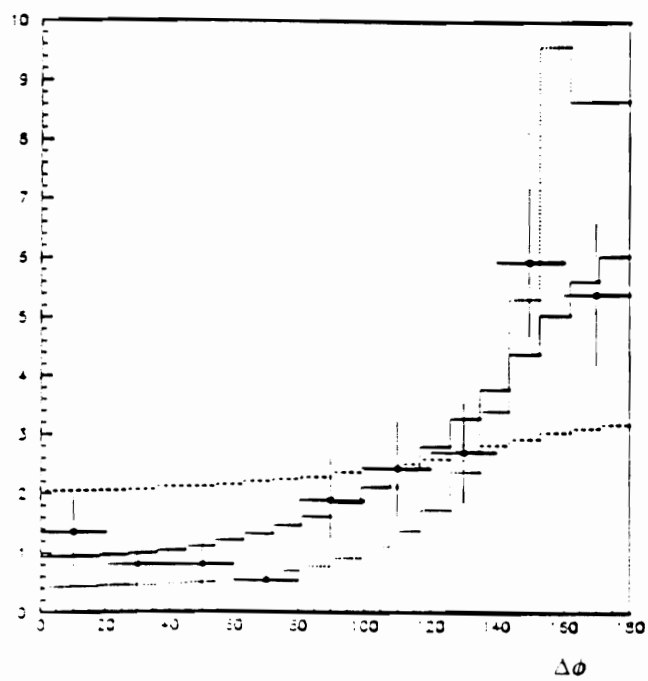

Fig. 3c

Fig. 3 - Acoplanarity angle.

a) Photoproduction: E687 data. The full line histogram is the NLO calculation;
b) Hadroproduction: NA32 data. The full line histogram is the NLO calculation;
c) Hadroproduction: WA92 data. Dotted line: NLO (Λ=330); full line: LO with $\sigma(p_t^2)_{gluon}$ =1(GeV/c)^2; dotted line: LO with $\sigma(p_t^2)_{gluon}$ =3 (GeV/c)^2.

2. Charmed Baryons

The most important results achieved in these last two years on charmed baryons, concern: the confirmation of the Ω_c, new decay channels of charged and neutral Ξ_c; Λ_c Cabibbo suppressed decays and Λ_c decays allowed by mechanisms different from a simple spectator. Mostly of them have been obtained by E687.

2.1 Ω_c^0

A first evidence for Ω_c^0, consisting of 3 events, has been obtained in 1985 by WA62[18] in the channel $\Xi^- K^- \pi^- \pi^-$ (mass = 2740±20 MeV).

In 1992 a confirmation was obtained by ARGUS[19] (12±7 events in the channel $\Xi^- K^- \pi^- \pi^-$; mass= 2719±7.7±2.5 MeV) and by E687[20] (10±4 events in the channel $\Omega^- \pi$; mass=2705.9±3.3±2.0 MeV). ARGUS has shown also evidence for the decay channel $\Omega^- \pi^- \pi^- \pi^-$ (6.5±3.2 events; mass: 2713±5.1 MeV)[21]. But no evidence for the two decay channels: $\Xi^- K^- \pi^- \pi^-$ and $\Omega^- \pi^- \pi^- \pi^-$ have been found by CLEO and E687 (these channels, compared with the $\Omega^- \pi$, have many more combinations falling into the expected signal region).

More recently E687 found evidence for Ω_c^0 into the decay channel

$$\Omega_c^0 \rightarrow \Sigma^- K^- K^- \pi^+$$

with Σ^- decaying both into $p\pi^-$ and $n\pi^-$. The analysis proceeded by identifying a kink between a microvertex track unlinked with a spectrometer track and a proton (π^+). $\check{C}$ identified , tracked in MWPC's of the spectrometer. From the proton (π^+) momentum and the kink angle it is possible to obtain the Σ^- momentum with a two fold ambiguity, via a zero constraint fit. The ambiguity can be solved chosing the best fit solution and, in some case, by means of the hadron calorimeter, which detects the secondary neutron. Due to the expected short lifetime, no detachment cut has been introduced, but only isolation cuts.

A preliminary sample of 34±7 events has been obtained, which is used to measure the Ω_c^0 lifetime. In Fig. 4a,b,c the two samples ($\Sigma^- \rightarrow p\pi^-$ and $\Sigma^- \rightarrow n\pi^-$) are plotted separately and superimposed each to other. In all three plots the mass and its σ are very well consistent each other (from the total sample $M_{\Omega_c} = 2698 \pm 1.59\ MeV$).

By means of a similar analysis procedure E687 obtained evidence also of the channel:

$$\Omega_c^0 \rightarrow \Sigma^- K^- K_s^0$$

(21.34±8.37 events) with a mass at 2709±3.7 MeV (see Fig. 5).

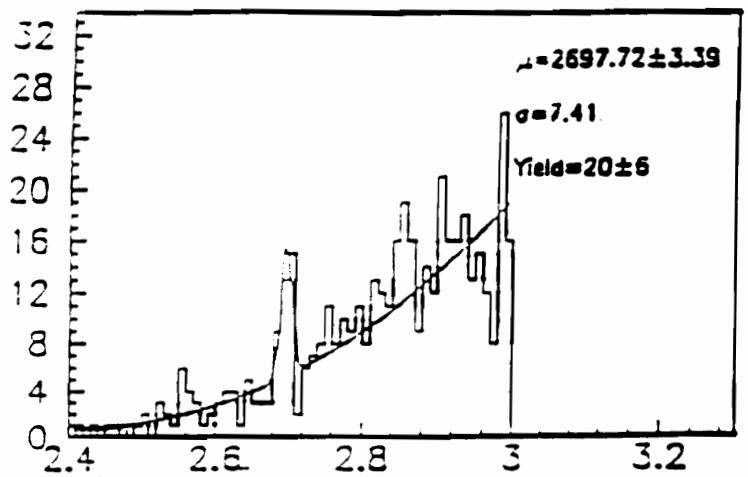

Fig. 4a

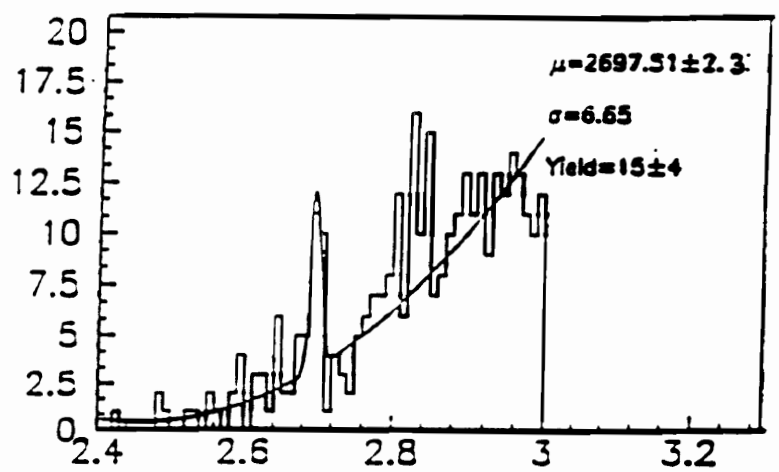

Fig. 4b

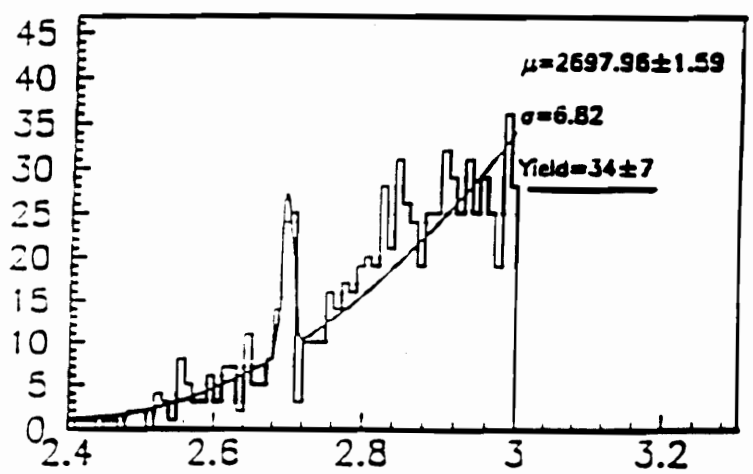

Fig. 4c

Fig. 4 - $\Sigma^- K^- K^- \pi^+$ mass plots.

a) sample with Σ^+ decaying to $p\pi^0$;

b) sample with $\Sigma^+ \rightarrow n\pi^+$;

c) total sample;

Even if we have presently several independent evidences for Ω_c^0, nevertheless the situation is not so confortable, because no one of the detected decay channels are found by two experiments (the WA62 evidence for $\Xi^- K^- \pi^- \pi^+$ is very week, consisting of only 3 events).

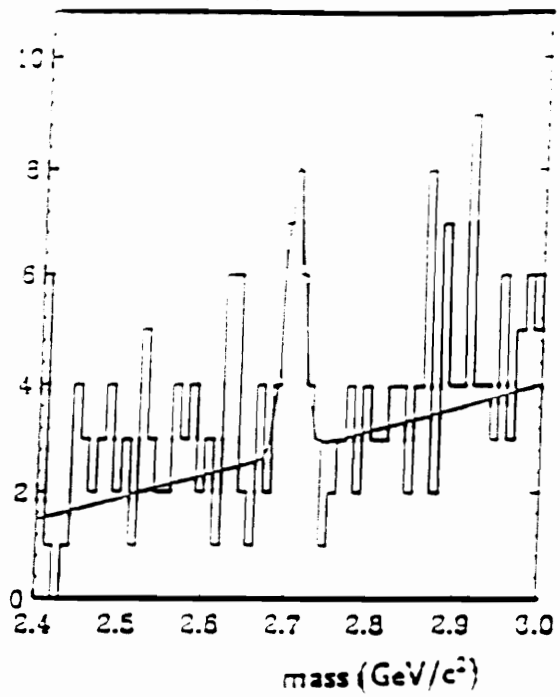

Fig. 5 - $\Sigma^- K^- K_s^0$ mass plot.

2.2 Ξ_c^+

The decay channel: $\Xi^- \pi^+ \pi^+$ ($\Xi^- \to \Lambda^0 \pi^-$; $\Lambda^0 \to p\pi^-$) has been studied by E687[22] and WA89[23]. The E687 analysis procedure accepts only Ξ^- decaying downstream the microvertex; then its track is reconstructed with high resolution by means of the microstrip detectors. The total sample consists of 29.7±7 events and it is used by E687 to measure the Ξ_c^+ lifetime.

The evidence obtained by WA89 is very good, but the mass shift of -15 MeV observed also in the channel $\Lambda^0 K^- \pi^+ \pi^+$), with respect to the nominal one, shows that some systematic bias is probably still present.

Evidences for further new channels are listed in Table V.

2.3 Ξ_c^0

The decay channel $\Xi_c^0 \to \Xi^- \pi^+$ has been studied by E687. The signal consist of 42±10 events and it has been obtained following an analysis procedure very similar to that adopted for Ξ_c^+ and described in 2.2. This sample is used by E687 to measure the Ξ_c^0 lifetime[24].

Further evidences are mentioned in Table V.

Table V

Channel	Experiment (s)	Signal
	Ξ_c^+	
$\Sigma^+K^-\pi^+$ $\Sigma^+ \to p\pi^0$	E687,	18.2±5.5 previously observed by NA32[26] with a signal consisting of 3 events
$\Sigma^+ \to n\pi^+$	E687	14±3
$\Lambda^0K^-\pi^+\pi^+$	E687	preliminary
	EXCHARM[25]	68/248
	WA89[23]	preliminary
$K^-K^0_S\pi^+\pi^+$	EXCHARM[25]	58/144
$\Omega^-K^-\pi^+$	E687	very preliminary
	Ξ_c^0	
Σ^+K^-	E687	20±8 (preliminary)
$\Sigma^+K^-\pi^+\pi^-$	E687	26±9 (preliminary)
$\Lambda^0K^{*0}(898)$	EXCHARM	50/61

2.4 Λ_c^+

I will mention here only five new measurements obtained by E687.

A signal of 14±6 events has been obtained by E687 studying the channel $\Sigma^+\delta(\Sigma^+ \to p\pi^0)$. A simple spectator mechanism is forbidden for this decay, which can go via a W-exchange.

The E687 analysis proceeded by searching for a kink between the microvertex track (not linked to any MWPC track) and an intersecting MWPC track (not linked to any microvertex track). The proton momentum and the kink angle allow the Σ^+ momentum to be determined with a two-fold ambiguity, which is solved using the confidence level.

The Branching Ratio has been measured with respect to the channel $\Sigma^+\pi^+\pi^-$, which goes via a normal spectator process. The result is:

$$\frac{B(\Sigma^+\delta)}{B(\Sigma^+\pi^+\pi^-)} = 0.16 \pm 0.086 \pm 0.048$$

in agreement with the Cleo determination[27].

The quoted number for this B.R. is relatively high. The contribution of final state interactions in the spectator process can be an hypothesis.

The Cabibbo suppressed decays: pK^-K^-, $p\pi^-\pi^-$, $p\pi^-\pi^-\pi^-\pi^-$, previously observed only by NA32 with very few events (4,4,3, respectively)[26], have been confirmed by E687[28].

In the selection of the decay $\Lambda_c^+ \to pK^-K^-$ a cut on $c\tau = \ell/\beta\gamma = \frac{lm}{p} < 5 \times c\tau_0 = 0.0323\ cm$ was adopted in addition to the usual detachment ($\ell/\sigma_\ell > 6$, and isolation cuts. The signal consists of 35.4 ± 10.3 events.

The Branching Ratio with respect to a Cabibbo allowed spectator process has been measured and the preliminary result is:

$$\frac{B(pK^-K^-)}{B(pK^-\pi^-)} = 0.096 \pm 0.029 \pm 0.010$$

A cut on ϕ mass allows to estimate the same B.R. for $\Lambda_c^+ \to p\phi$ ($\frac{B(p\phi)}{B(pK^-\pi^-)} < 0.58$: 90% C.L.).

The selection for the two further C.S. decays: $p\pi^-\pi^-$ and $p\pi^-\pi^-\pi^-\pi^-$ as been done by E687 requiring, in addition to the usual cuts, that $M(\pi^-\pi^-)$ and $M(p\pi)$ will be inconsistent with $M(K^0)$ and $M(\Lambda^0)$, respectively. The signals consist of 26 ± 9 ($p\pi^-\pi^-$) events and 40 ± 10 ($p\pi^-\pi^-\pi^-\pi^-$). The measurement of the B.R. are in progress.

3. Lifetime

The use of the "reduced proper time" and the choice of the "binned maximum likelihood" method are two important steps of the procedure followed in order to measure the lifetimes.

In the study of the heavy flavours the "detachment" cut ℓ/σ_ℓ is largely used as an important tool to disentagle the signal (ℓ is the distance in the space between primary and secondary vertices; σ_ℓ is its error). This cut distorts the exponential distribution of the measured proper time, which could be corrected by an heavy use of the Monte Carlo simulations. A better solution is to replace the proper time with the reduced proper time $t' = (\ell - N\sigma_\ell)/\beta\gamma c$, which nearly restores the exponential, thus minimizing the Monte Carlo corrections and then the systematic errors induced by the simulation. A distribution like $f(t')e^{-t'/\tau}$ is used in the fits, where $f(t')$ is a correction function, which takes into account the geometrical acceptance, the analysis cuts, the absorption in the target, the decay of charm secondaries.

Another important tool to minimize the systematic errors is the use of the binned maximum likelihood method which avoids a modelling of the background. Following this method, the t' distribution of the events present in two sidebands (data above and below the particle mass peak) are fitted and the result is used to determine the background underneath the signal.

The predicted number of events n_i in a t' bin is given by:

$$n_i = (N_S - B)\frac{f(t_i')e^{-t_i'/\tau}}{\Sigma f(t_i')e^{-t_i'/\tau}} + B\frac{b_i}{\Sigma b_i} \tag{3}$$

where s_i and b_i are the observed numbers of events in a t' bin i of the signal and of the side band histograms, respectively; N_S and B are the total number of events and the number of background events, respectively, in the signal region.

The relation between B and the background events expected from the side bands is assured by the factor ζ_{bg} included in the likelihood function.

The likelihood function is given by:

$$\zeta = \zeta_{signal} \times \zeta_{bg}, \tag{4}$$

where

$$\zeta_{signal} = \prod_{i=1} \frac{n_i^{s_i}}{s_i!}\exp(-n_i)$$

$$\zeta_{bg} = \frac{(n_{bg})^{N_{bg}}}{N_{bg}!}\exp(-\mu_{bg})$$

with : $N_{bg} = \Sigma b_i$ and $\mu_{bg} = B/R$; R is the ratio between the widths of the signal and sideband mass regions.

In the fit: τ and B are assumed as free parameters; $S = (N_s - B)$ is constrained to be the total number of signal events.

Using this procedure the background level is jointly determined in the same time by the invariant mass distribution and the t' evolution in the sidebands.

3.1 New lifetime measurements

New lifetime measurements have been obtained recently by E687 following the procedure described in the previous section.

In the E687 analysis the choice of the detachment cut does not influence significantly the fitted lifetime. In addition $f(t')$ introduces very small corrections: its value is very close to 1.1 and it is nearly flat in the full t' range. Just as an example, τ vs t/σ_t and $f(t')$ vs t' as obtained by E687 in the D_s analysis, are displayed in Figs. 6 and 7.

In the fitting, the signal region was defined within $\pm 2\sigma_m$, while the sidebands start $\pm\sigma_m$ above and below the mean D mass and their widths are within $2\sigma_m$.

The systematic effects have been studied very deeply, analyzing carefully: the absorption in the target (secondary elastic scattering can cause mismeasurements; the

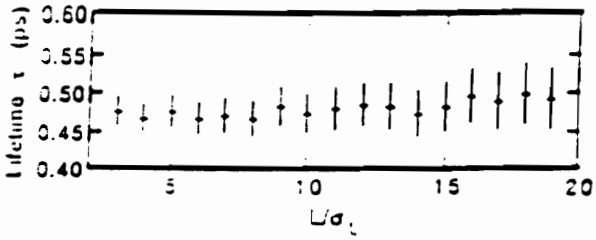

Fig. 6 - The fitted lifetime as a function of ℓ/σ_ℓ cut. The errors are statistical only.

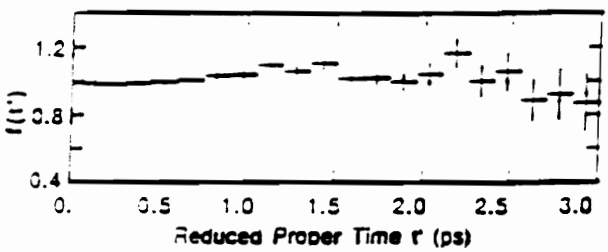

Fig. 7 - The correction factor $f(t')$ to the reduced proper time as function of reduced proper time.

corrections for secondary interactions suffer for cross section uncertainties); uncertainties in the acceptance calculation due to the modelling of the transverse beam profile, charmed states momentum distributions, choice of the sidebands, uncertainties in the $f(t')$ calculation, etc..

The results were always very reassuring: changements of the parameters, choices of the sample selection, different definition of the cuts can cause a variation of lifetime measured values always within $\pm\sigma_\tau$ around the quoted result of the analysis. Just as an example the D_s systematic studies done by E687 are shown in Fig. 8.

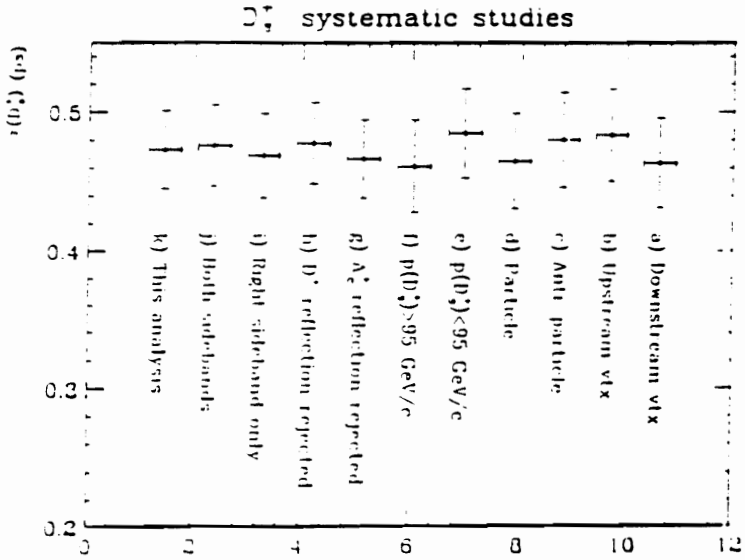

Fig. 8 - Study of the systematic effects for the D_s^+ lifetime measurements.

3.2 Results

The channels used by E687 to measure the lifetimes are listed in Table VI.

Table VI

State	Channel (all charged)	Total statistics
$D^{\pm}$	$K\pi\pi$	9189
$D^{0}, \overline{D^{0}}$	$K\pi$ $K\pi\pi\pi$ $K\pi\,(D^{*\pm}\ tag)$ $K\pi\pi\pi\,(D^{*\pm}\ tag)$	16730
$D_s^{\pm}$	$\phi\pi$ $\to K^{+}K^{-}$	900
Λ_c^{+}	$pK\pi^{+}$	1340
Ξ_c^{+}	$\Xi^{-}\pi^{+}\pi^{+}$	30
Ξ_c^{0}	$\Xi\pi$	42
Ω_c^{0}	$\Sigma KK\pi$ Σ^{-} $\to p\pi^{-}$ $\to n\pi^{+}$	~34

The results are quoted in Table III, where they are compared with the present world quotation.

Table VII

	E687 λ (psec)	PDG92 λ (psec)	Accuracy (E687)	Accuracy (PDG92)
$D^{\pm}$ [29]	$1.048 \pm .015 \pm .011$	$1.066 \pm .023$	1.8%	2.2%
D^{0} [29]	$.413 \pm .004 \pm .003$	$.420 \pm .008$	1.2%	1.9%
$D_s^{\pm}$ [30]	$.475 \pm .020 \pm .007$	$.450^{+.030}_{-.026}$	4.5%	6.7%
Λ_c^{+} [31]	$.215 \pm .016 \pm .008$	$.191^{+.015}_{-.012}$	8.3%	7.9%
Ξ_c^{+} [22]	$.410^{+.11}_{-.08} \pm .02$	$.30^{+.10}_{-.06}$	27.2%	33.3%
Ξ_c^{0} [24]	$.101^{+.025}_{-.017} \pm .005$	$.082^{+.059}_{-.030}$	25.2%	71.9%

The measurement of the Ω_c^{0} lifetime is still in progress. Very preliminary results gives a $\tau(\Omega_c^{0})$ comparable with the systematic error (~0.044 psec).

On the basis of the results of Table VII, E687 obtains:

$$\frac{\tau(D^{\pm})}{\tau(D^{0})} = 2.54 \pm 0.04 \qquad (5)$$

$$\frac{\tau(D_s^{\pm})}{\tau(D^{0})} = 1.15 \pm 0.05 \qquad (6)$$

The lifetime ratio (5) is consistent with the B. R. for the semileptonic decays, also obtained by E687:

$$\frac{B(D^{+} \to e^{+}x)}{B(D^{0} \to e^{+}x)} = 2.3^{+0.5+0.1}_{-0.4-0.1}$$

As it is well known explanations of the lifetime ratios (5) (6) are based upon the possible destructive interference of identical quarks in the $D^{\pm}$ final state (spectator diagram) and non negligible contributions of the exchange diagram (D^0) and the annihilation diagram $D_s^{\pm}$.

For what concerns the baryon hierarchy, E687 can quote:

$$\frac{\tau(\Xi_c^{+})}{\tau(\Lambda_c^{+})} = 1.91 \pm 0.44 \qquad (7)$$

and

$$\frac{\tau(\Xi_c^{0})}{\tau(\Lambda_c^{+})} = 0.47 \pm 0.11 \qquad (8)$$

The baryon hierarchy seems the following

$$\tau(\Xi_c^{0}) < \tau(\Lambda_c^{+}) < \tau(\Xi_c^{+}) \qquad (9)$$

From the very preliminary results obtained by E687 one could suppose that $\tau(\Omega_c^{0}) \leq \tau(\Xi_c^{0})$.

Previsions of the hierarchy can be obtained taking into account interferences (destructive and constructive) in the spectator diagram, exchange diagram contribution etc..[32,33].

4. Hadronic decays of charmed mesons

A large amount of new data are available in this field. I will restrict this report only to some open problems and to decay processes different from spectator.

4.1 $D^0 \to K^-K^+$ and $D^0 \to \overline{K^0}\pi^0$

These two decays represents a puzzle, whose solution is not yet fully settled.

The first concerns the ratio $R = \frac{B(D^0 \to K^-K^+)}{B(D^0 \to \pi^-\pi^+)}$. Both the K^-K^+ and $\pi^-\pi^+$ channels proceed via similar diagrams: spectator Cabibbo suppressed and exchange. On these bases the theoretical expectation is R=1.4.

The experimental situation is summarized in Table VIII. The last result obtained by E687 is in good agreement with CLEO and WA82, and in clear disagreement with the theoretical previsions.

Table VIII

Experiment	$\frac{B(D^0 \to K^-K^+)}{B(D^0 \to \pi^-\pi^+)}$
Mark II	3.4±1.8
Mark III	3.7±1.4
ARGUS[34]	2.5±0.7
CLEO[35]	2.35±0.37±0.28
E691[36]	1.95±0.34±0.22
WA82[37]	2.23±0.81±0.46
E687[38]	2.53±0.46±0.19

Possible explanations of this anomaly are based upon the significant role that final state interactions could play or on a possible interference between spectator and penguin diagrams, which should be positive for (K^+K^-) and negative for $(\pi^+\pi^-)$.

A second puzzle is connected to the D^0 decay into $\overline{K^0}\pi^0$. This decay is color suppressed, but the experimental determination of the B.R. with respect a decay channel allowed via an usual spectator process (as $D^0 \to K^-\pi^+$) is definitively much too high (see Table IX).

Table IX

Experiment	$B(D^0 \to \overline{K^0}\pi^0)/B(D^0 \to K^-\pi^+)$
Mark III[39]	0.45±0.10±0.10
CLEO[35]	0.55±0.06±0.07
E691[40]	1.36±0.23±0.22

The most recent result, obtained at fixed target by E691, is even higher than the previous ones (but the errors are also higher); it has been obtained by a sample of events D^* constrained (π^0's are reconstructed by the calorimeter; a cut on the angle between π^0 and D^* boost direction in the D^* r.f. is used to select the sample).

Soft gluon exchange, which should reduce the color suppression, could be a possible explanation of this result.

4.2 Decays to non strange states

The D and D_s can decay into non strange states, as 3π and 5π, via a Cabibbo suppressed spectator process (as in the case of $D^\pm$) and an annihilation diagram (as for $D_s^\pm$). In the case of D_s, the decay mechanism can be only a Cabibbo allowed annihilation process if the secondary particles do not give origin to resonant substructures, while a Cabibbo suppressed spectator mechanism gives contribution in case of a two body resonant final states.

Evidence for the $D^\pm, D_s^\pm$ decay to $\pi^\pm\pi^\pm\pi^\pm$ has been shown by E691[41] and E687. The mass plots are presented in Figs. 9a and 9b. In both spectra the misidentified $K\pi\pi$ reflection, the D and D_s peaks are clearly evident. The fitted yields consist of : 82.6±15.3 $D^\pm$ and 68.1±12.4 $D_s^\pm$ decays in the E691 sample; 179.2±21.1 $D^\pm$ and 54.2±12.3 $D_s^\pm$ in the E687 plot (in the E687 analysis the secondary vertex is required to be downstream the target; this condition is a strong tool in improving the signal to noise ratio).

Both the experiments proceeded to an analysis on the Dalitz plot: E691 uses an incoherent formalism while the E687 analysis, still in progress, is based upon the helicity formalism. In these types of analysis the background and its fluctuations are very crucial. As an example, the analysis of the D signal can be strongly influenced by the tail of the $K\pi\pi$ reflection.

The E691 results show that $(\pi^-\pi^-\pi^-)_{NR}$ and the $(f_0\pi^+)$ dominate the D_s decays and that their contribution are nearly equivalent. The B.R. between $D_s^\pm \to (\pi^\pm\pi^\pm\pi^\mp)_{NR}$ and a spectator Cabibbo allowed decay as $KK\pi$, can be a good indication of the contribution due to annihilation:

$$\frac{B(D_s^\pm \to \pi^\pm\pi^\pm\pi^\pm)_{NR}}{B(D_s^\pm \to K^-K^+\pi^\pm)} = 0.14 \pm 0.04$$

E687 found the first actual evidence of the D, D_s decay into 5π. Also in this case the requirement that the secondary vertex will be downstream the target gave an important help in disentangling the signal. The fitted yields (very preliminary) consist of 40±7 and 24±5 events for $D^\pm$ and $D_s^\pm$, respectively (see Fig 10).

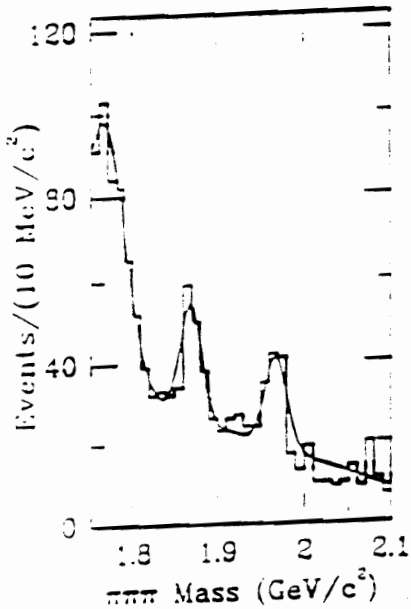

Fig. 9 (a)

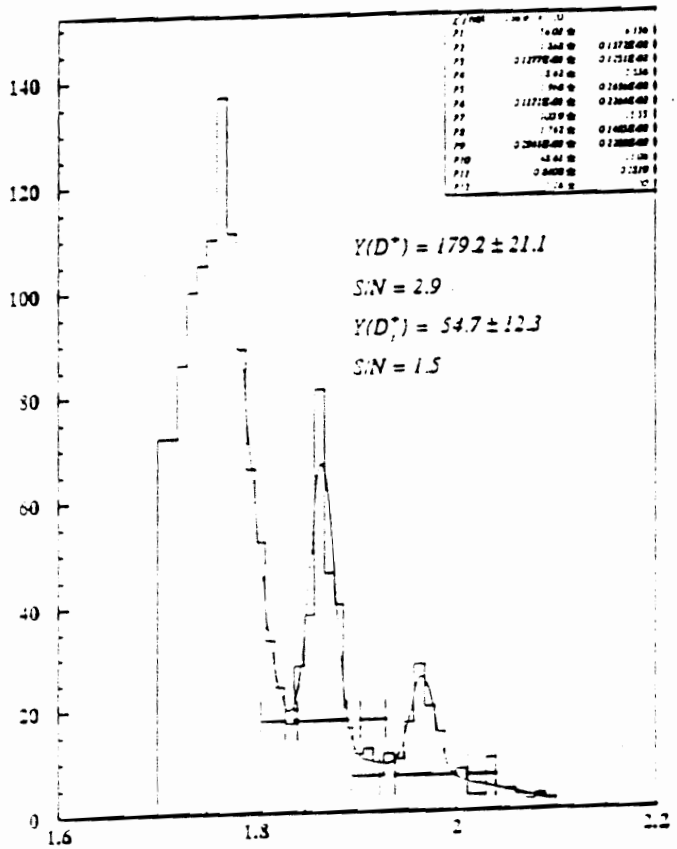

Fig. 9 (b)

Fig. 9 - 3 π mass distribution for the E691 sample (a) and E687 sample (b).

4.3 Search of substructures

E691[42] and E687[43] have recently analyzed the $K\pi\pi$ Dalitz plots, previously studied also by Mark III[44] and ARGUS[45]. The channels analyzed are: $D^{\pm} \to K^{\mp}\pi^{\pm}\pi^{\pm}$, $D^{0} \to K^{0}_{S}\pi^{+}\pi^{-}$, $D^{0} \to K^{-}\pi^{+}\pi^{0}$.

The analysis done by E687 was particularly complete because the formalism was extended to allow for the possibility of contributions from all known $(K\pi)$ and $(\pi\pi)$ resonances. The formalism is essentially based upon the Zemach method[46]. The high statistics allowed to adopt more severe cuts in the analysis, to reject phase space regions which could be contaminated by background channels , to D^{*} constraint the D^{0} samples.

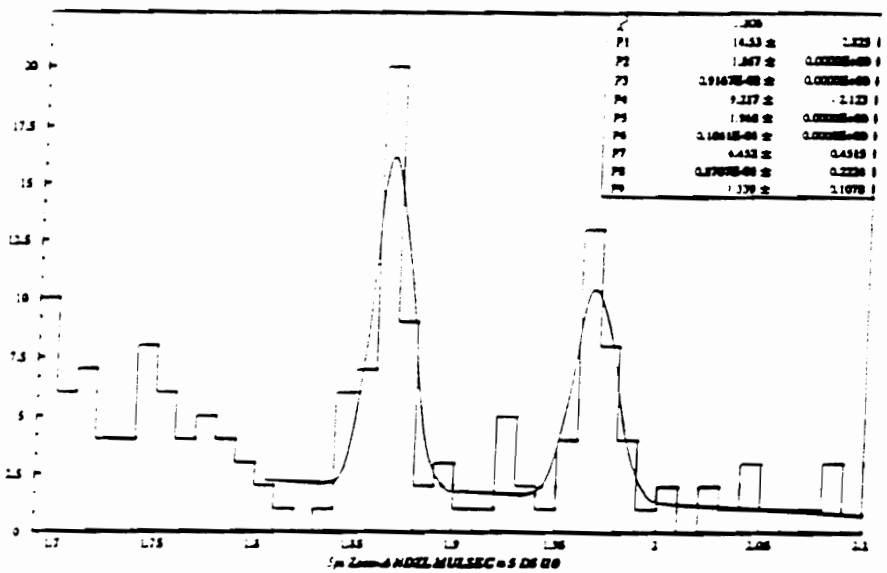

Fig. 10 - 5π mass plot (GeV).

The result is a very good signal to noise ratio (see Fig. 11). The fitted yields are: 8880±100 events for $D^{\pm} \to K^{\mp}\pi^{\pm}\pi^{\pm}$, 592±27 for $D^{0} \to K^{0}_{S}\pi^{+}\pi^{0}$ and 530±30 for $D^{0} \to K^{-}\pi^{+}\pi^{0}$.

There is a very good agreement between the results of E687 and ARGUS for $D^{0} \to K^{0}_{S}\pi^{+}\pi^{-}$, and a fair agreement among E687, E691 and Mark III for $D^{0} \to K^{-}\pi^{+}\pi^{0}$ and $D^{+} \to K^{-}\pi^{+}\pi^{+}$ (ARGUS does not analyze these two channels), even if some disagreement is present in the relative phase measurements.

The most important aspect of these results is the big difference of the non resonant contributions between D^{0} and $D^{\pm}$ channels; this is surprising because all three channels decay via similar diagrams. The $D^{0} \to K^{-}\pi^{+}\pi^{0}$ final states is well described by a sum of intermediate two-body resonances, without any appreciable contribution of non-resonant ; the $D^{0} \to K^{0}_{S}\pi^{+}\pi^{-}$ is approximately represented by intermediate two-body resonant decays with a small, but not negligible non-resonant contribution; the $D^{+} \to K^{-}\pi^{+}\pi^{+}$ decay mode, on the other hand, is characterized by a very large

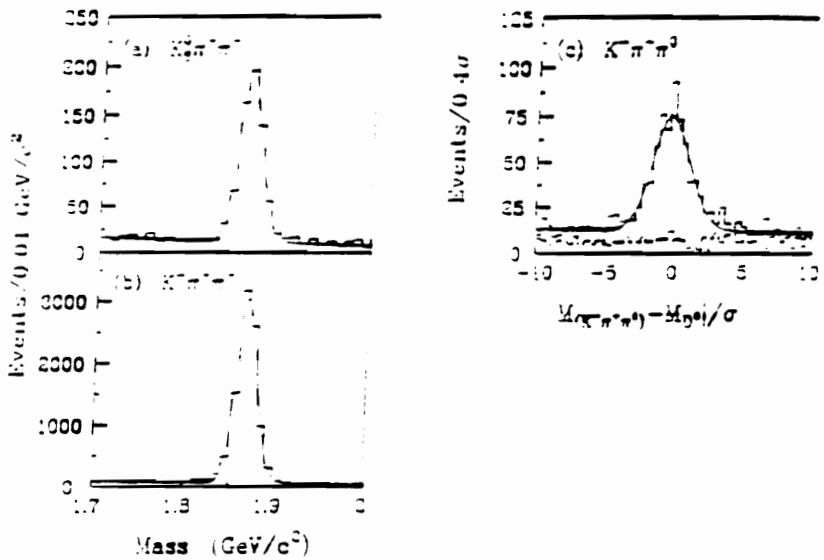

Fig. 11 - Mass plots (E687) of the samples of events for $K^0_s\pi^+\pi^-$, $K^-\pi^+\pi^-$, $K^-\pi^+\pi^0$.

non-resonant contribution, which strongly dominates the channel.

No clear explanation is presently available to understand these very different behaviours of $D^\pm$ and D^0 channels.

A Dalitz plot analysis of the $KK\pi$ channel is now in progress in the E687 collaboration making use of the helicity formalism. The D and D_s Dalitz plot projections and the relative fits are shown in Figs. 12a,b and 13a,b. The background is modelled across the Dalitz plot using directly the data from the sidebands.

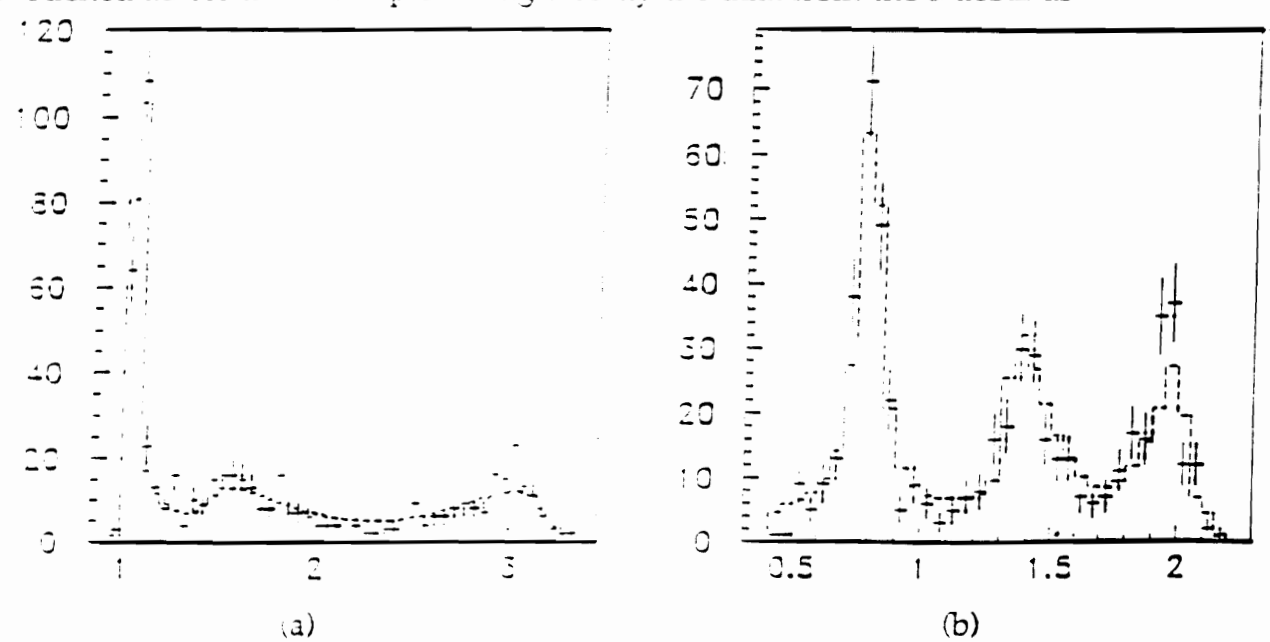

Fig. 12 - D_s^+ Dalitz plot $m^2_{K^-K^+}$ and $m^2_{K^-\pi^+}$ projections. The crosses are the experimental data and the histogram corresponds to the fit.

Performing a 3 amplitude fit (non-resonant, $\phi, \overline{K^{*0}}$), the D_s and D^+ decays show a different behaviour: while D_s is dominated by the two resonances with only a small

fraction of non-resonant events (~10%), the D^+ presents a large component of non-resonant events (~40%) comparable to the resonant fractions. When the f_0 (975) is introduced in the fit, part of the non-resonant events are attributed to this broad scalar resonance. Then the four amplitude fit is problematic due to the similarity of the f_0 and the non-resonant amplitudes on the Dalitz plot.

This is the first time that a full coherent Dalitz plot amplitude analysis has been performed on the $KK\pi$ final state.

The E687 three amplitude analysis seem to confirm previous measurements (E691)[47] to the extent of the D^+, but give a smaller non-resonant fraction in the D_s case.

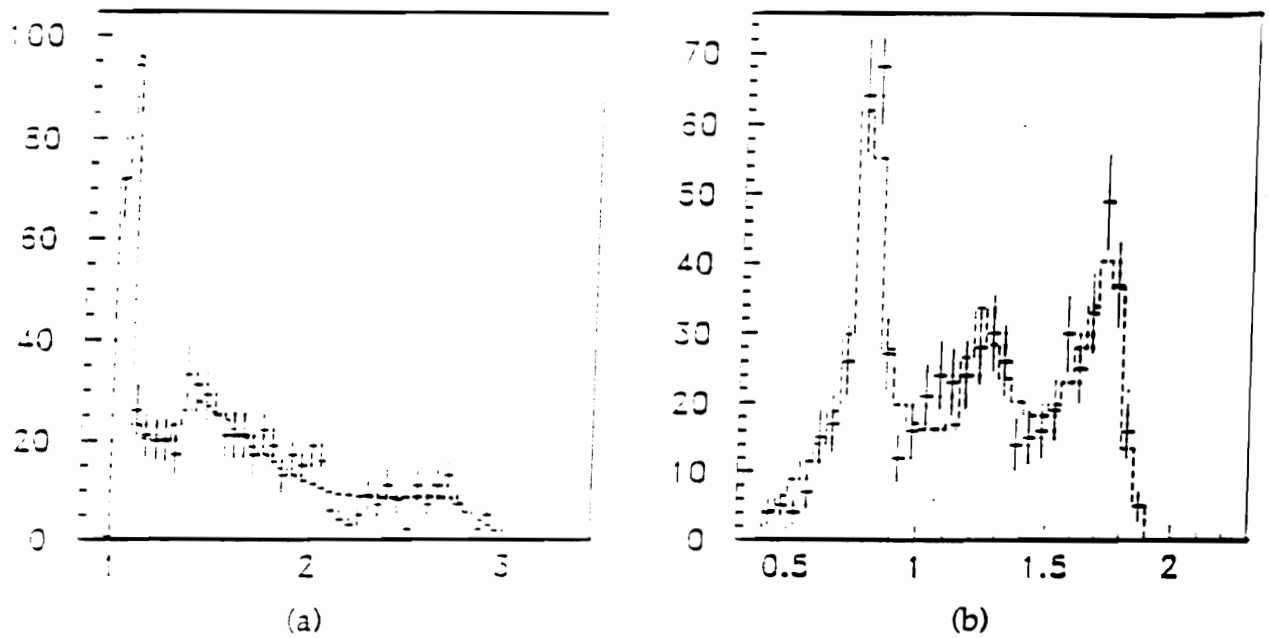

Fig. 13 - D^+ Dalitz plot $m^2_{K^-K^+}$ and $m^2_{K^-\pi^+}$ projections. The histogram corresponds to the fit and the crosses to the data.

5. Semileptonic decays of charmed mesons

As it is well known the semileptonic decays can be described by a simple spectator diagram, expressed by a product of hadronic and leptonic (point-like) currents. The point-like leptonic current is well know. The hadronic current is a function of q^2-dependent form factors, which describe coupling of meson wavefunctions to the virtual W.

The measurements of these form factors are of particular interest also because relations between them and the form factors for Beauty semileptonic decays are predicted by the Heavy Quark Effective Theory[48].

Few decay channels have been extensively studied by several experiments, included fixed target experiments. In the analysis of the semileptonic channels, due to the missed ν, the point back cuts are lost. Then further selections are used to identify the decays.

I will discuss here two channels and the form factors obtained from their analysis.

5.1 $D^0 \to K^- l \nu$

This channel has been studied by three experiments at fixed target: E691[49], E687[50] and E653[51]. For the D^0 sample E691 and E687 analyze only D^* tag events, make use of detachment and isolation cuts, impose $M_{Kl\nu} \equiv M_{D^0}$ to obtain p_ν, and finally do the selection on the $(M_{D^*} - M_D)$ plot. The D^* constraints are not used in the charged D sample. E653 uses the method of the "minimum parent mass" selecting decay $D^0 \to K^- \mu^+ \nu$ sample on this distribution by means of a maximum likelihood fit.

The results are shown in Table X, where they are compared with the MARK III[52] and CLEO[53] data. Two quotations are reported by E687, referred to two samples of data, collected in two different runs.

Table X

EXPERIMENTS	$BF(D \to \bar{K} \ell^+ \nu)$ (%)
	$D^+ \to \bar{K}^0 \ell^+ \nu$
MARK III (e)	$6.5 \pm^{1.6}_{1.1} \pm 0.7$
E691 (e)	$6.1 \pm 0.9 \pm 1.6$
Average	6.3 ± 1.2
	$D^0 \to K^- \ell^+ \nu$
MARK III (e)	$3.4 \pm 0.5 \pm 0.4$
CLEO (e)	$3.8 \pm 0.3 \pm 0.6$
CLEO (μ)	$3.3 \pm 0.3 \pm 0.6$
E691 (e)	$3.8 \pm 0.5 \pm 0.6$
E653 (μ)	$2.4 \pm 0.4 \pm 0.5$
E687(87-88) (μ)	$3.4 \pm 0.5 \pm 0.7$
E687(90) (μ)	$3.7 \pm 0.3 \pm 0.6$
Average	3.2 ± 0.4

There is a general agreement among the different results. Only the E653 measurement seems definitively lower than the other data.

The world weighted mean value of the semileptonic widths and the theoretical predictions are shown in Table XI[54]. The D^+ and D^0 experimental widths seem agree each other, within 2σ, as expected by the isospin symmetry.

The theoretical previsions are in general not very far from the measured values and for some model the agreement seems very good.

Table XI

Experimental widths
$\Gamma(D^+ \to \bar{K}^0 \ell^+ \nu) = 5.9 \pm 1.1 \;\; 10^{10}\, s^{-1}$
$\Gamma(D^0 \to K^{-0} \ell^+ \nu) = 7.7 \pm 0.8 \;\; 10^{10}\, s^{-1}$
$\Gamma(D \to \bar{K} \ell^+ \nu) = 7.1 \pm 0.6 \;\; 10^{10}\, s^{-1}$

THEORY	$\Gamma(D \to \bar{K}\ell^+\nu)$ $10^{10}\, s^{-1}$	$f_+(o)$	
QUARK MODEL			Reference
GS	7.1	0.69	Phys. Rev. D41 (1990) 142
WSB	8.26	0.76	Z. Phys. C29 (1985) 671
ISGW	8.5	0.76	Phys. Rev. D39 (1989) 799
KS	10.2(e)-9.9(μ)	0.76	Z. Phys. C46 (1990) 93
LATTICE GAUGE CALCULATION			
CMHS	9.5±4.	0.74±0.17	Phys. Lett. B223 (1989) 90
LMMS	5.8±1.5	0.63±0.08	Phys. Lett. B254 (1992) 415
BKS	12.±2.±5.	0.9±0.08±0.21	Phys. Rev. D43 (1991) 2140
QCD SUM RULES			
BBD	6.4±1.4	0.6±0.15	Phys. Rev. D44 (1991) 3567
DP	8.2±1.1	0.75±0.05	Phys. Lett. B207 (1988) 499
AEK	5.1±1.7	0.6±0.15	Sov. J. Nucl. Phys. 40 (1984) 527
AOS	9.1±4.5	0.8±0.2	IC-89-382 (1989)

For the D^+ decay to a pseudoscalar the width is:

$$\frac{d\Gamma}{dq^2} = \frac{G_F^2 |V_{cs}|^2 K^3}{24\pi^3} |f_+(q^2)|^2$$

where $K = \frac{M_D}{2}\left(1 - \frac{m_P^2 - q^2}{M_D^2}\right)^2 - \frac{4 m_P^2 q^2}{M_D^2}\Big]^{1/2}$ and $f_+(q^2)$ is the form factor.

The contribution of the terms involving the form factor $f_-(q^2)$ is negligible since they are multiplied by m_ℓ^2. For $f_+(q^2)$ the simple pole approximation is assumed $f_+(q^2) = \frac{f_+(0)}{1 - q^2/M_P^2}$. M_P is the pole mass of the nearest exchanged particle in the t channel (in this case the vector meson D_s^*).

The single pole mass value can be obtained by fitting the $\frac{d\sigma}{dq^2}$ vs q^2 shape. $f_+(0)$ can be measured by the width integrated over q^2 and assuming $|V_{cs}|=|V_{cd}|=0.9744$.

The results are shown in Table XII.

Table XII

Exp.	Mode	M_D	$\lvert f_+(0)\rvert$
E691	$K^-e^+\nu$	$2.1^{+0.4}_{-0.2}\pm0.2$	0.79 ± 0.05
E687	$K^-\mu^+\nu$	$2.1^{+0.7+0.7}_{-0.3-0.3}$	0.77 ± 0.08
CLEO	$K^-e^+\nu$	$2.1^{+0.4+0.3}_{-0.2-0.2}$	$0.77\pm0.01\pm0.04$
MARK III	$K^-e^+\nu$	$1.8^{+0.5+0.3}_{-0.2-0.2}$	

M_p is the best fit pole mass: it is in very good agreement with the D_s^* mass. The $f_+(0)$ weighted mean values[54] are: 0.73 ± 0.04 for D^0 and 0.64 ± 0.06 for D^+[55]. The average value for D^+ and D^0 is 0.7 ± 0.03, in a general good agreement with the theoretical expectations (Table XI).

5.2 $D^+\to\overline{K^{*0}}\ell\nu$ and $D^0\to(K^0_s\pi^-)^*\ell\nu$

The selection of these channels is done by E691[49] and E687[50] by identifying the $K\pi\ell$ combinations with right sign and by fitting the $K^-\pi^+$ and $K^-\pi^+\mu^+$ mass distributions with a fit function, which is a combination of the MC distributions of the signal and of the charm background decays. E653[51] uses the minimum parent mass to reject the contamination from decays with neutral products.

The ratios between the $(K^*\ell\nu)$ and the $(K\ell\nu)$ widths, as measured by various experiments, are shown in Table XIII, together with the signal yields and the world weighted mean values of $\Gamma(D^+\to\overline{K^{*0}}\ell^+\nu)$, $\Gamma(D^0\to K^{*-}\ell^+\nu)$ and $\Gamma(D\to\overline{K}\ell\nu)$[54]. The comparison of these results with the theoretical expectations of Table XIV confirms the well known disagreement with the quark models, which predict $D\to K^*\ell\nu$ widths and $\Gamma(D\to\overline{K}^*\ell\nu)/\Gamma(D\to\overline{K}\ell\nu)$ a factor two larger than the experimental data.

On the other hand the QCD sum rules seem to give previsions closer to the experimental measurements.

D decay to a vector particle introduces Lorentz invariant products of momenta and spins. Then the matrix element has to be written in terms of the three helicity amplitudes H_0, H_+ and H_- of the vector mesons:

$$\frac{d\Gamma}{dM_{K\pi}\cdot dt\cdot d\cos\vartheta_v\cdot d\cos\vartheta_\ell} = PS\times BW\times|M|^2$$

$$M = f\left[\cos\vartheta_\ell,\ \cos\vartheta_v,\ H_+(t),\ H_-(t),\ H_0(t)\right]$$

Table XIII

Experiment	Yield (events)	$\frac{\Gamma(D\to\overline{K}^*\ell\nu)}{\Gamma(D\to\overline{K}\ell\nu)}$
	$D^+\to\overline{K}^{*0}\ell^+\nu$	
MARK III (e)[52]		$1.0^{+0.3}_{-0.2}$
E691[49]	318	0.55±0.14
E653 (μ)[51]	305	0.43±0.09±0.09
E687 (μ)[50]	875	0.59±0.10±0.13
	$D^0\to K^{*-}\ell^+\nu$	
CLEO[53]		0.51±0.8±0.06
Average		0.55±0.07
$\Gamma(D^+\to K^{*0}\ell^+\nu=4.4\pm0.6\times10^{10}\ s^{-1}$ $\Gamma(D^0\to K^{*-}\ell^+\nu)=4.9\pm1.1\times10^{10}\ s^{-1}$ $\Gamma(D\to K^*\ell^+\nu)=4.5\pm0.5\times10^{10}\ s^{-1}$		

Table XIV

THEORY	$\frac{\Gamma(D\to\overline{K}^*\ell^+\nu)}{\Gamma(D\to\overline{K}\ell^+\nu)}$
QUARK MODEL	
GS	1.4
WSB	1.15
ISGW	1.1
KS	0.95
LATTICE GAUGE CALCULATIONS	
LMMS	0.86±0.27
QCD SUM RULES	
BBD	0.5±0.15
AOS	

where: ϑ_v is the angle between π and D in the K^* frame; ϑ_ℓ, between ℓ and D in the $\ell\nu$ r.f..

In the limit of massless leptons:

$$H_\pm = \alpha A_1(t) \pm \beta V(t)$$

$$H_0 = \delta A_1(t) - \varepsilon A_2(t)$$

$A_1(t)$ and $A_2(t)$ are the axial form factors; $V(t)$, the vector one. It is generally assumed that these form factors are given, in the one pole approximation, by: $F(t) = \frac{F(0)}{1 - t/M_p^2}$, with the vector pole given by the D_s^* mass (~2.1 GeV) and the two axial poles given by the D_s^{**} mass (~2.5 GeV).

Adopting the E691 convention, the experimental measurements are concentrated on $R_V = \frac{V(0)}{A_1(0)}$ and $R_2 = \frac{A_2(0)}{A_1(0)}$, which can be obtained by fitting the ϑ_v, ϑ_ℓ and t distributions.

The shape of the $\cos\vartheta_v$ intensity projection is controlled by the polarization parameter Γ_ℓ/Γ_t, e.i. the ratio of the longitudinal to transverse width of the virtual W:

$$\frac{d\Gamma}{d\Omega} \propto 1 + (2\frac{\Gamma_\ell}{\Gamma_t} - 1)\cos^2\vartheta_v,$$

The polarization parameter is a function of $|H_0|^2$ and $\{|H_+|^2 + |H_-|^2\}$. R_V and R_2 are very crucially influenced by the systematic errors; then the systematic effects due to the MC statistics, detector efficiency variations and background are studied very carefully.

The results are summarized in Table XV. The agreement between the E687[50] and the E653[51] is good, while discrepancies exists with the E691[49] measurement of R_2 and Γ_ℓ/Γ_t. The confidence level for an agreement among the three experiments on R_2 and R_V is 60%.

Table XV

Exp	R_2	R_V	Γ_ℓ/Γ_t
E691	$0.0 \pm 0.5 \pm 0.2$	$2.0 \pm 0.6 \pm 0.3$	$1.8^{+0.6}_{-0.4} \pm 0.3$
E653	$0.82^{+0.22}_{-0.33} \pm 0.11$	$2.00^{+0.33}_{-0.32} \pm 0.16$	$1.18 \pm 0.18 \pm 0.08$
E687	$0.78 \pm 0.18 \pm 0.10$	$1.74 \pm 0.27 \pm 0.28$	$1.20 \pm 0.13 \pm 0.13$
Average	0.74 ± 0.14	1.86 ± 0.2	1.21 ± 0.1

The comparison with the theoretical predictions reveal that there is a general disagreement between experiments and theory, with few exceptions (see Table XVI).

6.0 Limits on C.P. violation

A good signature for CP violation is an asymmetry in the decay rate of a charm decay mode and its CP conjugate.

Table XVI

THEORY	R_2	R_1	Γ_1/Γ_2
QUARK MODEL			
GS	0.8	1.9	1.2
WSB	1.3	1.4	0.9
ISGW	1.0±0.3	1.4±0.4	1.1±0.2
KS	1.0	1.0	1.1
LATTICE GAUGE CALCULATIONS			
LMMS	0.36±0.4	1.6±0.2	1.51±0.27
BKS	0.7±0.3	2.0±0.4	
QCD SUM RULES			
BBD	1.2±0.2	2.2±0.9	0.86±0.06
AOS	0.89±0.39	1.89±0.79	

In order to produce such an asymmetry, we need two independent weak decay amplitudes, which contribute to the same final state (as Cabibbo suppressed decays or decay with mixing). In addition, final state interactions must induce a phase shift between the two decay amplitudes.

A good channels should be $D^0 \to K^-K^+$, which can be compared with $\overline{D^0} \to K^+K^-$. The charge of the D^* daughter π is used to divide the D^0 by the $\overline{D^0}$ sample. To measure the asymmetry we use the parameter:

$$A_{cp} = \frac{\eta(D) - \eta(\overline{D})}{\eta(D) + \eta(\overline{D})}$$

η is the $D, \overline{D}$ decay channel yield, normalized to a $D, \overline{D}$ Cabibbo allowed channel, as $\eta(D) = \frac{N(D^0 \to K^+K^-)}{N(D^0 \to K^-\pi^+)}$ and $\eta(\overline{D}) = \frac{N(\overline{D^0} \to K^-K^+)}{N(\overline{D^0} \to K^+\pi^-)}$. The normalization is needed to take into account the different D and $\overline{D}$ rates.

E691 and E687 have searched for CP violation, using the procedure described above. The measured limits are: $|A_{cp}(K^+K^-)|$<45% (90% Conf. Level) from E691[56] and <13% from E687[57] (90% Conf. Level).

E687 studied also the decay channel $D^0 \to K^-K^+\pi^+$, by using $D^+ \to K^-\pi^+\pi^+$ as normalization channel. Here the situation is complicated by the possible intermediate resonant states. The CP asymmetry could be different for each decay mode, since the strong phase shift and the relative size of the two weak decay amplitudes vary.

E687 studied the $K^{*0}K^+$ and $\phi\pi^-$ contributions, analysing the $K^{\pm}\pi^{\mp}$ and K^+K^- invariant mass distributions.

The measured limits (90% Conf. Level) are the following:

$A_{cp}(K^-K^+\pi^+)_{total} < 10\%$ $\quad A_{cp}(K^{*0}K) < 22\%$ $\quad A_{cp}(\phi\pi) < 12\%$

7.0 Conclusions

i) Good improvements have been achieved in these last years in understanding the production mechanisms. Fairly large samples of double tag events are now becoming available, allowing correlation studies. In the meantime a big effort has been done by the theoreticians to calculate the NLO corrections for the gluon-gluon and photon-gluon models.

ii) The charmed meson lifetimes are very well known, with very small statistical and systematic errors. We are very close to fix the lifetime hierarchy for the charmed baryons.

iii) The Ω_c^0 mass is established quite well. Unfortunately no decay channel has yet been observed by two different experiments.

iv) Measurements of charmed baryon decay channels, Cabibbo suppressed or allowed by exchange processes, are becoming to be available.

v) The good statistics now reached in meson decay processes, different from a simple spectator, is starting to allow a more quantitative study of the non-dominant diagrams.

vi) In semileptonic decays, the decay transition pseudoscalar-pseudoscalar seems now understood. The decay process pseudoscalar-vector shows discrepancies with the theoretical expectations.

References

1) S. Frixione et al., Nucl. Phys. B 412 (1994) 225 NuPhA
2) M.L. Mangano et al., Nucl. Phys. B 405 (1993) 507 NuPhA
3) P. Nason et al., Proc. of the Advanced Study Conference on "Heavy Flavours", Pavia, September 1993, Ed. Frontieres. In press
4) G. Ridolfi et al., Proc. of the Workshop "Heavy Quarks at fixed target", Frascati (1993) p. 81
5) M.L. Mangano et al., Nucl. Phys. B373 (1992) 295 NuPhA
6) M.P. Alvarez et al., CERN-PPE/92-28
7) J.C. Anjos et al., Phys. Rev. Lett. 62 (1989) 513 PRLTA; J.C. Anjos et al., Phys. Rev. Lett. 65 (1990) 2503 PRLTA
8) S. Kwan, Proc. of the Advanced Study Conference on "Heavy Flavours". Pavia, Sept. 1993, Ed. Frontieres. In press
9) P. Nason, private communication
10) G.A. Alves et al., Phys. Rev. Lett. 69 (1992) 3147 PRLTA
11) M. Adamovich et al., Phys. Lett. B305 (1993) 402 PhLTA
12) G.A. Alves et al., Phys. Rev. Lett. 72 (1994) 812 PRLTA
13) G.A. Alves et al., Fermilab, Pub. 93/081-E
14) M. Adamovich et al., Phys. Lett. B 284 (1992) 453 PhLTA
15) G.A. Alves et al., Phys. Rev. Lett. 70 (1993) 722 PRLTA
16) L. Rossi, private communication
17) P.L. Frabetti et al., Phys. Lett. B308 (1993) 193 PhLTA
18) S.F. Biagi et al., Z. Phys. C23 (1985) 175 ZEPYA
19) H. Albrecht et al., DESY preprint 92-052
20) P.L. Frabetti et al., Phys. Lett. B300 (1993) 190 PhLTA
21) J. Stiewe (ARGUS Coll.). Production and decays from ARGUS. XXVI ICHEP (Dallas, 1992), unpublished
22) P.L. Frabetti et al., Phys. Rev. Lett. 70 (1993) 1381 PRLTA
23) S. Brons et al., Proc. of the Workshop "Heavy Quarks at Fixed Target", Frascati (1993) p. 181
24) P.L. Frabetti et al., Phys. Rev. Lett. 70 (1993) 2038 PRLTA
25) D. Kekelidze, Proc. XXVI ICHEP (Dallas 1993) p. 1066
26) S. Barlag et al., Z. Phys. C48 (1990) 29 ZEPYA
27) P. Avery et al., CLEO-93-04 (1993)
28) P.L. Frabetti et al., Phys. Lett. B314 (1993) 477 PhLTA
29) P.L. Frabetti et al., Phys. Lett. B323 (1994) 459 PhLTA
30) P.L. Frabetti et al., Phys. Rev. Lett., 71 (1993) 827 PRLTA
31) P.L. Frabetti et al., Phys. Rev. Lett., 70 (1993) 1755 PRLTA
32) B. Guberina et al., Z. Phys. C33 (1986) 297 ZEPYA
33) M.B. Voloshin et al., Sov. Phys. JETP 64 (1986) 698 SPHJA
34) H. Albrecht et al., Z. Phys. C46 (1990) 9 ZEPYA
35) J. Alexander et al., Phys. Rev. Lett. 65 (1990) 1184 PRLTA
36) J.C. Anjos et al., Phys. Rev. D44 (1991) R3371 PhRVA
37) M. Adamovich et al., Phys. Lett. B280 (1992) 163 PhLTA
38) P.L. Frabetti et al., Phys. Lett. B321 (1994) 295 PhLTA
39) J. Adler et al., Phys. Rev. Lett. 60 (1988) 89 PRLTA
40) J.C. Anjos et al., Phys. Rev. D46 (1992) R1 PhRVA
41) J.C. Anjos et al., Phys. Rev. Lett. 62 (1989) 125 PRLTA

42) J.C. Anjos et al., Phys. Rev. D48 (1993) 56 PHRVA

43) P.L. Frabetti et al., Analysis of the three $D \to K\pi\pi$ Dalitz plots, to be published in Phys. Lett. B

44) J. Adler et al., Phys. Lett. B196 (1987) 107 PHLTA

45) H. Albrecht et al., Phys. Lett. B308 (1993) 435 PHLTA PHRVA

46) C. Zemach, Phys. Rev. 133 (1964) B1261; C. Zemach, Phys. Rev. 140 (1964) B109

47) J.C. Anjos et al., Phys. Rev. Lett. 60 (1988) 897 PRLTA

48) N. Isgur et al., Phys. Lett. B237 (1990) 527 PHLTA

49) J.C. Anjos et al., Phys. Rev. Lett. 62 (1989) 1587; Phys. Rev. Lett. 62 (1989) 722; Phys. Rev. Lett. 65 (1990) 2630; Phys. Lett. 67 (1991) 1507; Phys. Rev. Lett. 64 (1990) 2885

50) P.L. Frabetti et al., Phys. Lett. B307 (1993) 262; Phys. Lett. B315 (1993) 203; Phys. Lett. B313 (1993) 253 PHLTA

51) K. Kodama et al., Phys. Rev. Lett. 66 (1991) 1819; Phys. Lett. B286 (1992) 187; Phys. Lett. B274 (1992) 246

52) Z. Bai et al., Phys. Rev. Lett. 66 (1991) 1011 PRLTA

53) G. Crawford et al., Phys. Rev. D44 (1990) 3394; J.A. Alexander et al., Phys. Rev. Lett. 65 (1990) 1531 PRLTA

54) E. Meroni, Proc. of the Workshop "Heavy quarks at fixed target" Frascati (1993), p. 151

55) R. Gardner, Proc. of the Advanced Study Conf. on "Heavy Flavours", Pavia (1993) Ed. Frontieres. In press

56) J.C. Anjos et al., Phys. Rev. 44 (1991) R3371 PHRVA

57) P.L. Frabetti et al., Search for CP violation in charm meson decay, submitted to Phys. Rev. Lett.